JOURNAL OF SOLID STATE CHEMISTRY 41, 90–96 (1982)

Solid Solubility of Ge, Si, and Mg in Fe_2O_3 and Photoelectric Behavior

H. L. SANCHEZ,* H. STEINFINK,* AND H. S. WHITE†

Materials Science and Engineering Laboratories, Department of Chemical Engineering, and †Department of Chemistry, The University of Texas at Austin, Austin, Texas 78712

Received July 20, 1981; in revised form September 18, 1981

Solid solutions of GeO_2 in Fe_2O_3 were prepared by mechanically mixing the solids and firing at 1000°C in air, and from a gel obtained by the addition of an alcohol solution of germanium ethoxide to iron dissolved in HNO_3. The dried gel was then heated at 1000°C. The solubility limit is 5 mole% GeO_2, $Fe_{1.95}Ge_{0.05}O_3$. Similar procedures were used to prepare solid solutions with Si and the solubility limit is greater than 4 mole% SiO_2. Firing of mixtures or gels of Fe_2O_3 containing Mg produces a spinel phase even at the lowest detectable concentrations. The resistivity of pressed pellets of $Fe_{2-x}Ge_xO_3$ varies from about 10^6 ohm-cm for $x = 0$ to about 10^{-1} ohm-cm for $x = 0.05$. The photoassisted electrolysis of water at Ge-doped Fe_2O_3 electrodes is demonstrated. The Fe_2O_3(Ge)/0.7 *M* $Fe(CN)_6^{4-}$, 0.05 *M* $Fe(CN)_6^{3-}$/Pt photoelectrochemical cell showed a 0.29-V open-circuit voltage, 1.2-mA/cm² short-circuit current, 0.31 fill factor, and 0.06% power efficiency.

Introduction

Iron oxide, α-Fe_2O_3, has been studied extensively as an anode for the photodecomposition of water (*1–7*). Its value of the band gap energy of 2.2 eV is nearly ideal for optimum absorption of solar energy for this purpose but the electrical resistivity and other required electrical characteristics of pure iron oxide are unsuitable. The crystal structure of α-Fe_2O_3 consists of close-packed layers of oxygen ions and two of the three available octahedral interstices are occupied by Fe^{3+}. Isomorphous replacement of iron by other transition metals can be easily achieved and the introduction of higher or lower valent atoms should produce a mixed valence state and alter the electrical behavior of the material. Studies have been carried out in which Ti (*6, 8*), Sn and Ca (*9*), Cu and Al (*8*), Cr (*3*), and recently Si (*10*) have been introduced into α-Fe_2O_3. The introduction of tetravalent ions, e.g., Ti^{4+} produces n-type material, whereas the substitution of Ca^{2+} produces p-type behavior (*11*). The introduction of Mn, Cr, and Cu are reported to give n-type behavior, while Mg and Ni produce p-type behavior (*12*). The electrical characteristics of pure α-Fe_2O_3 can also be modified by heating it at high temperatures to produce a nonstoichiometric material but these results are suspect because of the probable formation of Fe_3O_4 on the surface of the particles (*3, 13*). The replacement of Fe^{3+} by other transition metals to modify the electrical behavior is fraught with uncertainty because of the variable valence states that these elements can assume.

Tetravalent germanium and silicon can

0022-4596/82/010090-07$02.00/0

be substituted for iron, and a study using Ge^{4+} has been reported by Patterson who found that a solid solution between GeO_2 and Fe_2O_3 forms up to 3.24 wt% GeO_2 (*14*). He proposed that the reaction proceeds by substitution of iron as follows:

$$(1 - x/2)Fe_2O_3 + xGeO_2 \rightarrow Fe_{2-x}Ge_xO_3 + (x/4)O_2. \quad (1)$$

If the proposed mechanism is correct then the substitution should be accompanied by weight loss up to the maximum range of solid solubility. It is also conceivable that a cation could be placed into the vacant octahedral site and modify the physical properties by such a procedure. In this study we report the determination of the extent of solid solution of Ge and Si in α-Fe_2O_3, the measurement of the electrical and photoelectrical properties of the doped materials, and the results when Mg^{2+} is introduced into the structure.

Experimental

Solid solutions were prepared by two methods: (1) mechanically mixing the reactants in powdered form and firing at 1000°C in air; (2) preparation of a gel with subsequent firing at 1000°C.

Powdered mixtures were prepared from commercially obtained materials having at least 99.9% stated purity. The reagents were first preheated to constant weight at 1000°C. The dried materials were weighed using a microbalance, suspended in alcohol and ground in an agate mortar for 20–150 min. The mixture was placed either in alumina or platinum crucibles, dried to constant weight at 140–180°C and transferred to a furnace and reacted at 1000°C. The weight loss during the reaction was monitored by shutting off the furnace in 1- or 2-day intervals, allowing the sample to cool in a desiccator and after having reached room temperature, weighing the sample on a microbalance. This cycle was repeated until either a constant weight or a constant daily weight loss was achieved. It took from 2 to 4 weeks to reach such a stage in the reaction. Platinum crucibles were found to lose a small amount of weight continuously at 1000°C and the weight losses were corrected for this effect.

In the gel technique metallic iron was dissolved in hot HNO_3, the solution was cooled to 0°C and the ethoxides of Ge or Si, dissolved in ethanol, were added. Upon neutralization with NH_4OH an amorphous gel formed. The excess liquid was evaporated over a water bath, the gel dried at 60–70°C and then fired at 1000°C. The subsequent procedures were as previously described.

Electrical resistivity measurements were done on sintered pellets using the van der Pauw four-probe method (*15, 16*). The pellets were prepared by grinding the reacted mixtures in an agate mortar, cold pressing up to 70,000–100,000 psi, and sintering at 1000 to 1300°C for up to 4 days. Contacts to the pellets were made by attaching copper wires against the circumference using silver paint. The density of the pellets was obtained from weight and volume measurements; the latter calculated from micrometer or microscopic measurements of thickness and diameter. Densities were also obtained from liquid displacement measurements using ethanol. These two techniques do not yield the same values. Physical measurements of volume will include the pore structure of the material. Such measurements yielded values ranging between 66–84% of the density of pure Fe_2O_3, 5.24 g/cm^3, while the liquid displacement method gave values of 94% or higher.

All powder X-ray diffraction diagrams were obtained with a diffractometer equipped with a diffracted beam monochromator and Cu$K\alpha$ radiation.

The photoelectric response of these materials was studied by using them as anodes

in a photochemical cell. The electrodes were prepared by sanding pellets sintered at 1300°C with SiC sandpaper of grades 180, 320, and 600, followed by ultrasonic cleaning in ethanol. Pellets sintered at lower temperatures were also used as electrodes but showed unstable photoelectric behavior. Contacts were made by rubbing indium–gallium alloy into the back of the pellets which were then contacted with conductive silver paint to a copper wire. The electrode was subsequently sealed in epoxy and silicon rubber so as to leave only one side exposed. A platinum foil counter electrode and a saturated calomel electrode (SCE), as reference electrode, were used. All electrochemical measurements were performed with a PAR Model 173 potentiostat (Princeton Applied Research Corp.) controlled by a PAR model 175 universal programmer. Current–potential curves were recorded on an x–y recorder. A 450-W Xenon lamp (focused power = 150 mW/cm^2) was used as the source of illumination.

Results

A plot of the experimental weight loss at 1000°C for the GeO_2–Fe_2O_3 system vs mole% GeO_2 and the expected curve based on Eq. (1) is shown in Fig. 1. The weight loss increases until the concentration of GeO_2 reaches 4.89 mole%, corresponding to $x = 0.05$ in Eq. 1. Further additions of GeO_2 did not produce additional weight loss. The solid-solution limit found in these experiments agrees well with the value reported by Patterson (*14*). Up to 3 mole% GeO_2 the weight loss curve follows the calculated curve very closely, but thereafter a small deviation occurs, which could be due to experimental errors in the determination of the completion of the reaction or the incorporation of additional oxygen in the lattice to compensate for the tendency of α-Fe_2O_3 to be slightly oxygen deficient (*11*). X-Ray diffraction powder patterns of the

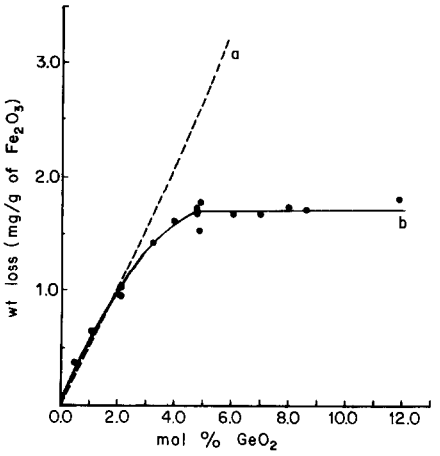

FIG. 1. Weight loss of reacted mixtures of Fe_2O_3 and GeO_2 as a function of molar concentration of GeO_2 in unreacted mixture (mg/g of Fe_2O_3 in mixture). (a) Calculated, based on Eq. (1). (b) Experimental.

solid solutions confirm the solubility limit to be between 4.8 and 4.9 mole% GeO_2. When the concentration of GeO_2 exceeded this value, GeO_2 diffraction lines began to appear in the patterns. Identical results were also seen for specimens prepared from gels.

We investigated the possible preparation of $Fe_{2-x}Ge_xO_3$ by reacting $FeGeO_3$ and Fe_2O_3 in evacuated Vycor tubes at 1000°C. It was thought that a mixture of $FeGeO_3$ and Fe_2O_3 might react as follows:

$$x\mathrm{FeGeO_3} + (1 - x)\mathrm{Fe_2O_3} \rightarrow \mathrm{Fe_{2-x}Ge_xO_3}. \quad (2)$$

When the solid-solution range is exceeded, the additional phases that might be expected would be $Ge_{1.8}Fe_{3.2}O_8$ and Fe_3O_4 (*17*). However, the detection of the Fe_3O_4 spinel phase is quite difficult because of the superposition with many of the peaks from the other phases and no definite conclusions as to the range of solid solubility could be obtained by this technique. Kimizuka (*18*) has studied the reaction

$$(1 - 2x)\mathrm{Fe_2O_3} + x\mathrm{GeO_2} + x\mathrm{Fe_3O_4} \rightarrow \mathrm{Fe_{2-x}Ge_xO_3} \quad (3)$$

and found x to be less than 0.075 at 1000°C by thermogravimetric methods.

Mixtures of SiO_2 and Fe_2O_3 were prepared as previously reported and fired at 1200°C. Powder X-ray diffraction patterns indicated the presence of some unreacted SiO_2 in every product. Mixtures prepared by the gel method using $Si(C_2H_5O)_4$ as the source of the silicon did not show SiO_2 lines even at concentrations of 4% Si. Apparently the reaction does not go to completion when mixtures prepared by mechanical grinding of Fe_2O_3 and SiO_2 are used.

Attempts to produce Fe_2O_3 doped with Mg by reacting with metallic Mg or MgO were not successful. In all cases either the unreacted MgO or a spinel phase, probably $MgFe_2O_4$, was present. However, a gel prepared by dissolving Fe and Mg metals in HNO_3 in the molar ratio 1 : 0.020, drying at 100°C and firing at 400°C showed only lines due to α-Fe_2O_3. At higher firing temperatures the spinel phase appeared. It is possible that a solid solution exists at the lower temperatures but this has not been confirmed. All attempts to prepare $Fe_{2-x}Mg_xO_3$ at 1000°C always resulted in the formation of a spinel phase even at very low values of x.

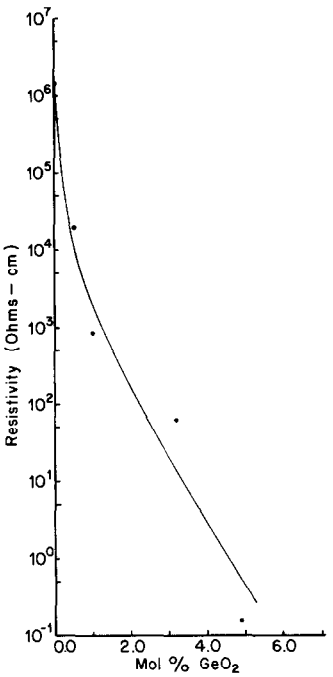

FIG. 2. Electrical resistivity of doped Fe_2O_3 as a function of concentration of GeO_2 (mole%, based on total GeO_2 + Fe_2O_3), reacted at 1000°C.

Electrical Resistivity and Photoelectric Behavior

Figure 2 shows the electrical resistivity as a function of concentration of GeO_2. This curve agrees qualitatively with the results of Patterson (*14*) up to the solid-solution limit. However, since the resistivity measurements were made on polycrystalline materials, absolute values cannot be expected to coincide.

Beyond the solid-solution limit, the resistivity is expected to increase due to the presence of a second phase, GeO_2. Therefore, we believe that one should not show a cusp in the resistivity curve as shown by Patterson, as this could incorrectly suggest the presence of a phase transition. X-Ray diffraction patterns of mixtures of higher concentration than the solubility limit showed only α-Fe_2O_3 and GeO_2 (hexagonal). We found the resistivity of mixtures containing between 10 and 15% GeO_2 to be roughly independent of composition with a value around 435 ohm-cm.

Figure 3 shows the voltammetric response of an iron oxide electrode doped with 0.1% GeO_2 in 1.0 *M* NaOH solution (degassed with prepurified N_2 to remove O_2). The onset potential of photocurrents was −0.2 V vs SCE with a net photocurrent density of 0.1 mA/cm² measured at +0.3 V. Current densities as high as 1 mA/cm² were obtained at this doping level. The onset potential of photocurrents shifts to more negative values by ~59 mV/pH unit over the pH range 7–14, with relatively small difference in current density, as expected for the photoassisted electrolysis of water. This

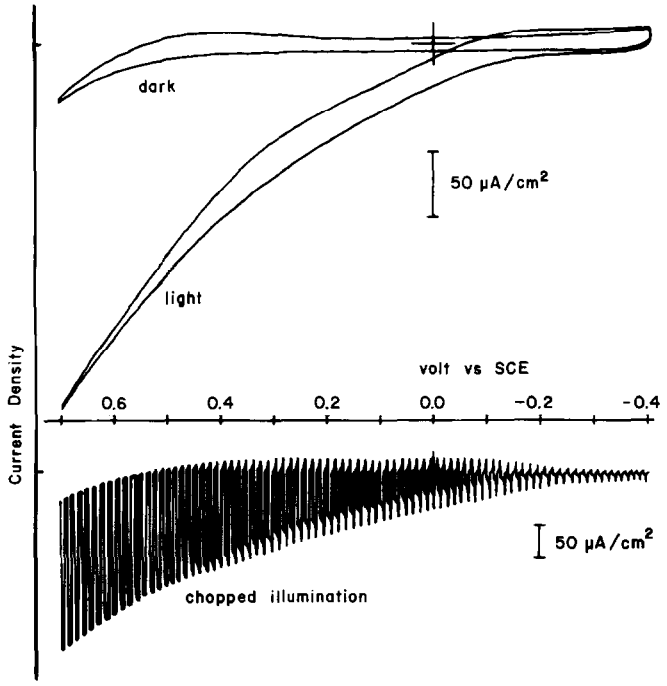

FIG. 3. Current density vs potential for Fe_2O_3 electrode doped with 0.1% GeO_2 in 1.0 *M* NaOH solution.

result is similar to previous results obtained at chemically vapor deposited α-Fe_2O_3 films on Pt (*1*), although the photocurrents were approximately one order of magnitude lower.

Comparable photocurrents were obtained in 0.7 *M* $Fe(CN)_6^{-4}$, 0.05 *M* $Fe(CN)_6^{-3}$ (pH 9.1 borate buffer) solution, Fig. 4. The onset potential of photocurrents was -0.1 V vs SCE. Since the redox potential of $Fe(CN)^{-4/-3}$ is 0.25 V vs SCE, the photounderpotential for the oxidation of $Fe(CN)_6^{-4}$ is ~0.35 V. The photocurrent density for this electrode was 1.1 mA/cm² at 0.3 V in $Fe(CN)_6^{-4/-3}$ solution. No change in the photocurrents was observed when the electrodes were returned to NaOH solutions, indicating that chemical etching of the electrode surface had not taken place.

A photoelectrochemical cell (PEC) based on the photooxidation of $Fe(CN)_6^{-4}$ was constructed to test the efficiency of the Ge doped Fe_2O_3 photoanode. Figure 5 shows the i–V curve (the electrode cell with no external power supply) obtained by measuring the voltage drop across a variable-load resistor between the photoanode and a Pt counter electrode (10 cm²). The open-circuit photovoltage and short-circuit photocurrent were 0.29 V and 1.2 mA/cm², respectively. The power conversion efficiency of α-Fe_2O_3 (0.1% Ge)/Fe $(CN)_6^{-4/-3}$/Pt PEC was ~0.06% (input power ~150 mW/cm²).

Silicon-doped iron oxide anodes produced smaller photocurrents. The maximum net photocurrent obtained at +0.3 V vs SCE was 9 μA/cm². The efficiency of a cell using this anode was not measured.

The resistivity of the 0.1% GeO_2 electrode was about 3×10^4 ohm-cm, while that of 0.1% SiO_2 was greater than 10^6 ohm-cm. The density of these electrodes was greater than 80%, based on physical measurement

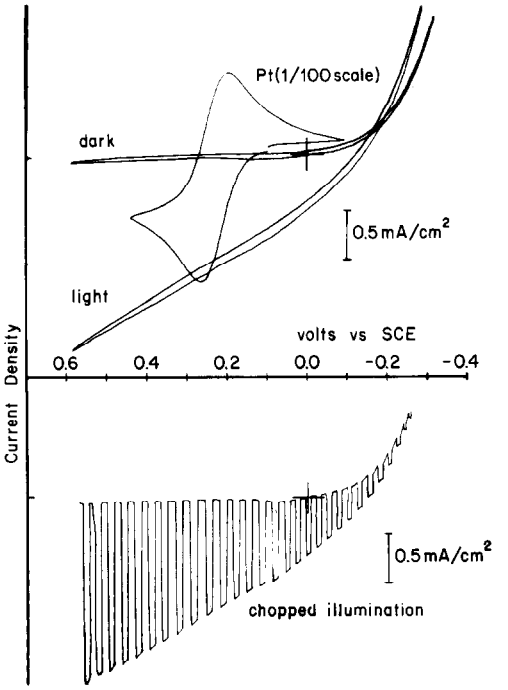

FIG. 4. Current density vs potential for Fe_2O_3 electrode doped with 0.1% GeO_2 and for Pt electrode in 0.7 *M* $Fe(CN)_6^{-4}$, 0.05 *M* $Fe(CN)_6^{-3}$ (pH 9.1 borate buffer).

of the volume, and greater than 97%, based on liquid displacement.

Mg-doped iron oxide has not been tested for photoelectric response because at 400°C well-sintered pellets cannot be obtained, and at higher temperatures a spinel phase forms as was previously discussed.

Undoped iron oxide prepared under the same conditions showed negligible dark currents and photocurrents.

From these results we conclude that, although polycrystalline iron oxide doped with Si or Ge behaves as a photoanode in a photoelectrochemical cell, the currents obtained are too small for practical applications at the present time.

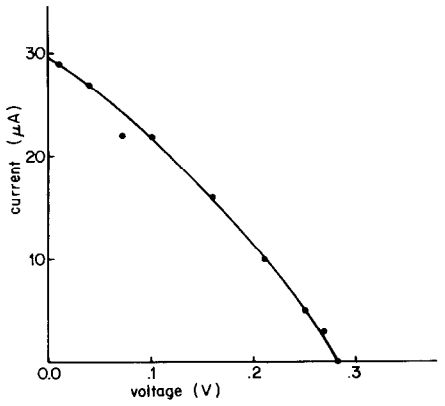

FIG. 5. Current voltage characteristics of α-Fe_2O_3(Ge)/$Fe(CN)_6^{-4/-3}$/Pt PEC. Photoanode area ≈ 0.03 cm². Fill factor: 0.31. Illumination: 450-W xenon lamp.

Acknowledgments

This research was supported by a grant from the R. A. Welch Foundation, Houston, to H. L. S. and H. S., and NSF Grant CHE 80-00682 to H. S. W. We also wish to thank Dr. Kimizuka, National Institute for Research in Inorganic Materials, Ibarakiken, Japan, for many stimulating exchanges of ideas.

References

1. K. L. HARDEE AND A. J. BARD, *J. Electrochem. Soc.* **123,** 1024 (1976).
2. R. K. QUINN, R. D. NASBY, AND R. J. BAUGHMAN, *Mater. Res. Bull.* **11,** 1011 (1976).
3. P. MERCHANT, R. COLLINS, R. KERSHAW, K. DWIGHT, AND A. WOLD, *J. Solid State Chem.* **27,** 307 (1979).
4. L. R. YEH AND N. HACKERMAN, *J. Electrochem. Soc.* **124,** 833 (1977).
5. H. H. KUNG, H. S. JARRETT, A. W. SLEIGHT, AND A. FERRETTI, *J. Appl. Phys.* **48,** 2463 (1977).
6. J. H. KENNEDY AND K. W. FRESE, JR., *J. Electrochem. Soc.* **125,** 709 (1978).
7. J. S. CURRAN AND W. GISSLER, *J. Electrochem. Soc.* **126,** 56 (1979).
8. R. C. JOB AND P. J. KELLEHER, Final Report October 1978 to U.S. Department of Energy, Solar Energy. Available from NTIS, Document No. C00-4546-6, U.S. Department of Commerce, Springfield, Virg. 22161.
9. M. GORI, H. R. GRÜNIGER, AND G. CALZAFERRI, *J. Appl. Electrochem.* **10,** 345 (1980).
10. J. H. KENNEDY, R. SHINAR, AND J. P. ZIEGLER, *J. Electrochem. Soc.* **127,** 2307 (1980).
11. G. H. GEIGER AND J. B. WAGNER, JR., *Trans. Metal. Soc. AIME* **233,** 2092 (1965).

12. R. F. G. GARDNER, F. SWEET, AND D. W. TANNER, *J. Phys. Chem. Solids* **24,** 1175 (1962).
13. J. H. W. DEWIT AND A. I. BROERSMA, *J. Solid State Chem.* **37,** 242 (1981).
14. F. K. PATTERSON, U.S. Patent 3,890,251, June 17, 1975.
15. L. J. VAN DER PAUW, *Philips Res. Rep.* **13,** 1 (1958).
16. L. J. VAN DER PAUW, *Philips Tech. Rev.* **20,** 220 (1958).
17. E. TAKAYAMA, N. KIMIZUKA, K. KATO, H. YAMAMURA, AND H. HANEDA, *J. Solid State Chem.* **38,** 82 (1981); private communication with N. Kimizuka.
18. N. KIMIZUKA, private communication,